Thermal Decomposition of Alkaline-Earth Metal Hydride and Ammonia Borane Composites

Yu Zhang, Keiji Shimoda, Hiroki Miyaoka, Takayuki Ichikawa*, Yoshitsugu Kojima

Institute for Advanced Materials Research, Hiroshima University, 1-3-1 Kagamiyama, Higashi-Hiroshima 739-8530

*Corresponding author: T. Ichikawa, Email: tichi@hiroshima-u.ac.jp

Abstract

We demonstrate a method to improve the promising hydrogen storage capabilities of ammonia borane by making composites with alkaline-earth metal hydrides using ball-milling technique. The ball-milling for the mixtures of alkaline-earth metal hydride (MgH_2 or CaH_2) and ammonia borane (AB) yields a destabilization compared with the ingredient of the mixture, showing the hydrogen capacity of 8.7 and 5.8 mass% at easily accessible dehydrogenation peak temperatures of 78 and 72 °C, respectively, without the unwanted by-product borazine. Through detailed analyses on the dehydrogenation performance of the composite at various ratios in the hydride and AB, we proposed a different chemical activation mechanism from that in the LiH/AB and NaH/AB systems reported in a previous literature.

Keywords: Hydrogen; Ammonia borane; Alkaline-earth metal hydride; Dehydrogenation; Borazine

1. Introduction

With fossil fuel reserves running low and energy demand rising, the search for alternative fuels is a matter of great importance [1-2]. Hydrogen as a secondary energy is generally considered as the most ideal fuel from the comprehensive clean energy concept [3-5]. For the on-board application of hydrogen energy as a transportation fuel, one of the most important technological challenges is the discovery and development of safe and economically viable solid-state storage materials for hydrogen [6-8]. However, two major obstacles for a widespread use of hydrogen especially for mobile applications have proven to be critical: hydrogen production and hydrogen storage [9]. Since storing pure hydrogen is out of question for a variety of reasons (volumetric energy density), one of the key steps on the road to a working hydrogen economy will be the development of an efficient hydrogen storage material. The volumetric density of compressed hydrogen or the liquefied temperature of liquid hydrogen are considered too "low" for transport applications [1] and many researchers consider chemical hydrides as a more viable alternative [6].

Ammonia borane (AB, NH_3BH_3), contains ~19.6 mass% hydrogen, and has been considered as a hydrogen storage material [10-11]. Hydrogen is generated in three stages when tetragonal ammonia borane is heated, with a single equivalent of hydrogen evolved in each stage at ca. 110, 150, and 400-900 °C in temperature ramping experiments [12-14]. The first equivalent hydrogen can also be released at temperatures as low as 70 °C in isothermal experiments, but only after a long induction period. However, only ~6.3 mass% can be released in the temperature range

of 70-120 °C, indicating it would be inapplicable to meeting with the DOE's 2015 target for a successful on-board hydrogen storage system (9.0 mass% of pure hydrogen easily released up to 85 °C) [15].

Several approaches, including use of various transition metals and base-metal catalysts [16], acid catalysis [17], particle size effects from nanoscaffolds [18], ionic liquids [19], and carbon cryogels [20-21], etc., have been reported to improve the dehydrogenation properties of AB in terms of the reduced dehydrogenation temperatures, accelerated H_2 release kinetics, and/or minimized byproduct like borazine release [16-19]. Recent efforts to modify the kinetics and thermodynamics of H_2 release from AB have been made by replacing one H with an alkali metal [22-23], i.e., $LiNH_2BH_3$ and $NaNH_2BH_3$, and alkaline-earth metal hydrides [24-28], which shows a significant enhance of dehydrogenation kinetics and a suppressed borazine release. These amidoboranes release large amount of hydrogen with no measurable borazine formation. Based on these efforts to develop this novel chemical activation approach, we further extended the destabilizer scope to alkaline-earth metal hydrides. In this work, we found that mechanically milled AB with alkaline-earth metal hydrides (MH_2, M = Mg and Ca) can also dramatically improve the dehydrogenation kinetics of AB.

2. Experimental details

The starting material MgH_2, CaH_2 (purity 95 %) and ammonia borane (NH_3BH_3, AB, purity 90%) were purchased from Sigma-Aldrich Co. Ltd. These materials were used as-received without any purification. All the samples were handled in an argon

glovebox purified by a gas recycling purification system (MP-P60W, Miwa MFG Co., Ltd.) to minimize the oxygen and water content.

The MgH_2/AB and CaH_2/AB samples were prepared by ball-milling alkaline-earth metal hydrides with ammonia borane in a molar ratio of 1:1 (total 300 mg) under Ar atmosphere (0.1 MPa) for 10 h by using stainless steel vial and 20 steel balls with diameter of 7 mm in a planetary mill apparatus (Fritsch 7) at 370 rpm. The ball to powder weight ratio is 100:1. Other alkaline-earth metal amidoboranes were prepared in the same procedure by ball-milling AB with the corresponding alkaline-earth metal hydrides at various molar ratios.

The gas desorption behaviors of all the products were examined by thermal desorption mass spectroscopy measurements (TDMS, M-QA200TS, Anelva; detection limit: $1e^{-11}$ nA) combined with thermogravimetry (TG; TG8120, Rigaku). The heating rate is 1 °C min^{-1} and the helium gas flow speed is 300 mL min^{-1}. The structure of samples was characterized by X-ray diffraction measurement (XRD; RINT-2100, Rigaku, CuKα radiation). The Fourier transform infrared spectroscopy (FT-IR; Spectrum One, Perkinelmer) measurements were performed by using a diffuse reflection cell to examine IR active stretching modes of powder samples in the as-milled alkaline-earth metal amidoboranes products. For FT-IR measurements, all the samples were diluted by potassium bromide (KBr) down to 10 mass%. Additionally, the FT-IR equipment is also installed inside a home-made glove-box filled with purified argon gas.

3. Results and discussion.

Fig. 1 showed the thermal decomposition behaviors of the AB composites with MgH_2 or CaH_2 by using TG-TDMS at temperatures up to 120 °C with a heating rate of 1 °C min^{-1}. Neat AB releases about 6.3 mass% of H_2 in the temperature range of 70-120 °C and requires an initial induction period of around 30 min at 100 °C prior to hydrogen release, as reported in the previously results [6]. Compared to neat AB, mechanically milling AB with alkaline-earth metal hydride can significantly improve the dehydrogenation properties, such as lower dehydrogenation temperature and enhanced dehydrogenation quantity. MgH_2/AB began to release hydrogen at as low as 50 °C and most of hydrogen was released at 78 °C. The fact that ball mill MgH_2 and CaH_2 can lower the temperature of hydrogen release is very similar to the results from a recent work [28]. However, at present, we can not obtain any solid evidence about the chemically or physically react of MgH_2 or CaH_2 react with AB. Totally 8.7 mass% of hydrogen based upon added AB and MgH_2 were evolved at temperatures below 120 °C. It should be noted that, although a small amount of ammonia was detected during the dehydrogenation process, the ammonia emission was not synchronized with hydrogen desorption peak. Unlike the solvent-containing $Ca(NH_2BH_3)_2{\cdot}2THF$, which releases organic molecules in addition to hydrogen, solvent-free CaH_2/AB mixtures show a cleaner desorption profile with definite hydrogen desorption temperature [29]. CaH_2/AB mixtures start to desorb hydrogen at ~45 °C with vigorous hydrogen release at ~72 °C and ~88 °C. Mass loss begins at temperatures as low as 55 °C with *ca.* 5.8 mass% total loss up to 120 °C. It should be noted that only trace

ammonia was detected throughout the decomposition process of the CaH_2/AB sample compared with MgH_2/AB mixture, indicating this specific sample holds satisfactory performance in suppressing the volatile by-products, i.e. there is no unwanted by-product borazine in the released gas. The peculiar performance of the two samples may attribute to the stronger ionicity of Ca^{2+} than Mg^{2+}, which can affect the crystal and electronic structure of AB and efficiently suppress the release of NH_3. This is of significantly importance for its application in fuel cell.

The powder X-ray diffraction (XRD) pattern for samples is shown in Fig. 2. Both the ball milling alkaline-earth metal hydride and AB mixtures are typical of a multicomponent system. For ball milled mixture of MgH_2/AB and CaH_2/AB, all peaks can be indexed to NH_3BH_3 and corresponding metal hydride. The result seems to show that metal hydride does not react with the NH_3BH_3 during the milling process, which is different from the reported $LiNH_2BH_3$ and $NaNH_2BH_3$ compounds [22-23]. XRD on the products of these alkaline-earth metal hydride/AB mixtures after desorption indicated formation of amorphous phases, which prevents direct determination of their structure. The diffraction peaks of MgH_2 and CaH_2 can just be identified in the post-heating products together with the amorphous phases. The amorphous phase might be considered as a $(BN)_x$ polymer for its high crystallization temperature (1000 °C). These results indicated that the products after dehydrogenation of alkaline-earth metal hydride/AB mixtures mainly included alkaline-earth metal hydride, amorphous $(BN)_x$, and H_2.

The IR spectra measured for the ball-milled samples consists of several strong

absorption bands in the NH bending (1380 cm^{-1} and 1600 cm^{-1}), BH bending (1060 cm^{-1} and 1170 cm^{-1}) and BH stretching region (2335 cm^{-1}) and few less intense bands in the NH stretching region (3270 cm^{-1}) as shown in Fig. 3. The dramatic decay of intensity of the bands in the NH stretching and NH bending region is seen upon thermal decomposition of MgH_2/AB and CaH_2/AB mixtures. This is accompanied by a much less pronounced decrease of the bands assigned to BH stretching and BH bending modes.

Besides this excellent MH_2/AB (M = Mg, Ca) samples, other nonstoichiometric alkaline-earth metal amidoboranes also exhibit superior dehydrogenation performance in compared with pristine AB. For instance, ball-milled MgH_2/2AB, MgH_2/3AB, and MgH_2/9AB samples show vigorous hydrogen release at about 88, 92, and 108 °C, respectively (Fig. 4). And ball-milled CaH_2/2AB, CaH_2/3AB and CaH_2/9AB samples show vigorous hydrogen release at about 82, 85, and 87 °C, respectively (Fig. 4). It should be pointed out the beginning of decomposition temperatures of nonstoichiometric calcium amidoboranes are lower than 55 °C, which is much lower than the onset dehydrogenation temperatures of LiAB (90 °C) and NaAB (87 °C). Notably, another visible peak was observed to centre at around 113 °C, which correspond to the decomposition steps yielding excess of AB [10-12]. The excess of AB can decrease the dehydrogenation temperature and increase the mass of the released gas, most of which attributed to the thermolysis of the excessive AB. However, the gas was not pure hydrogen, and composed most hydrogen and a little ammonia. These findings clearly indicate that the *M*H/AB (*M* = Mg, Ca) systems

involve a different chemical activation mechanism from that in the LiH/AB and NaH/AB systems reported in literature [22-23].

Mechanically milling AB with alkaline-earth metal hydride provides a simple and effective approach to destabilize AB for hydrogen storage application. The improved dehydrogenation properties of these products have been ascribed to the presence of both positive (protonic) and negative (protidic) hydrogen and avoidance of mass transport trough different phases as for the amide-hydride combination. The changes in the reaction kinetics reflect the different reactivity of hydrogen in the alkaline-earth metal hydride and AB mixtures. The existence of a stronger electron-donating alkaline-earth metal will induce considerable changes in the electronic state of N with concomitant modification of the chemical bonding between B and N. With more electrons being donated from alkaline-earth metal to NH_3BH_3, the degree of the hydridic B-H bond of NH_3BH_3 is thus increased, which enhance its activity compared to those in solid AB. As a consequence, the chemical bonding of B-N, B-H and N-H will be affected. More importantly, the present study demonstrates that the hydrogen release reaction of AB can be made less exothermic by simple substitution of H in the NH_3 group by Li^+ cation [22-23]. This finding provides a new promising way to tune the problematic thermodynamics of AB, and to pursue the potential of fulfilling the hydride regeneration via solid-gas reaction. In addition, the existence of alkaline-earth ions, NH_3BH_3 molecules created more polar surroundings compared to the solid AB. Compared to reactions between NH_3BH_3 in solid AB, the polar environments of MgH_2/AB and CaH_2/AB mixtures coupled with a change in the reactivity among

these ions in the alkaline-earth metal hydride and AB mixtures will facilitate B-H and H-N interactions between the adjacent NH_3BH_3 molecules. This kind of activation role might be responsible for the observed easier release of H_2.

4. Conclusions

We have shown that ball milling alkaline-earth metal hydride and AB mixtures yields a destabilized hydrogen storage material with hydrogen capacity 8.7 mass% and 5.8 mass% at easily accessible dehydrogenation temperatures without the unwanted by-product borazine. These materials offer significant advantages over their parent compound, ammonia borane. This research work, safe, economical, hydrogen-rich storage materials, meet the challenge in the move towards a hydrogen-based energy economy.

Acknowledgment

Financial support from the New Energy and Industrial Technology Development Organization (NEDO) within the project of “Advanced Fundamental Research on Hydrogen Storage Materials” is kindly acknowledged.

References

[1] Züttel A. Hydrogen storage and distribution systems. Mitig Adapt Strat Glob Change 2007;12:343–65.

[2] Zhang XB, Yan JM, Han S, Shioyama H, Xu Q. Magnetically recyclable Fe@Pt core−shell nanoparticles and their use as electrocatalysts for ammonia borane oxidation: the role of crystallinity of the core. J Am Chem Soc 2009; 131(8):2778-79.

[3] Schlapbach L, Züttel A. Hydrogen-storage materials for mobile applications. Nature 2001; 414:353–8.

[4] Momen G, Hermosilla G, Michau A, Pons M, Firdaouss M, Hassouni K. Hydrogen storage in an activated carbon bed: effect of energy release on storage capacity of the tank. Int J Hydrogen Energy 2009; 34(9):3799–808.

[5] Lee TB, McKee ML. Mechanistic study of $LiNH_2BH_3$ formation from $(LiH)_4$ + NH_3BH_3 and subsequent dehydrogenation. Inorg Chem 2009;48(16):7564–75.

[6] Stowe AC, Shaw WJ, Linehan JC, Schmid B, Autrey T. In situ solid state ^{11}B MAS-NMR studies of the thermal decomposition of ammonia borane mechanistic studies of the hydrogen release pathways from a solid state hydrogen storage material. Phys Chem Chem Phys 2007, 9(15):1831-6.

[7] Song SY, Zhang Y, Xing Y, Wang C, Feng J, Shi WD, Zheng GL, Zhang HJ. Rectangular $AgIn(WO_4)_2$ nanotubes: a promising photoelectric material. Adv Funct Mater 2008;18(16):2328–34.

[8] Tambvekar SV, Subrahmnyam M. Photocatalytic generation of hydrogen from hydrogen sulfide: An energy bargain. Int J Hydrogen Energy 1997; 22(10-11):959-65.

[9] Yang XJ, Cheng FY, Liang J, Tao ZL, Chen J. Pt_xNi_{1-x} nanoparticles as catalysts for hydrogen generation from hydrolysis of ammonia borane. Int J Hydrogen Energy 2009;34(21):8785–91.

[10] Stephens FH, Pons V, Baker RT. Ammonia–borane: the hydrogen source par excellence? Dalton Trans 2007;25:2613-26.

[11] Pons V, Baker RT, Szymczak NK, Heldebrant DJ, Linehan JC, Matus MH, Grant DJ, Dixon D. Coordination of aminoborane, NH2BH2, dictates selectivity and extent of H2 release in metal-catalysed ammonia borane dehydrogenation. Chem Commun 2008:6597–99.

[12] Bowden M, Kemmitt T, Shaw W, Hess N, Linehan J, Gutowski M, et al. Mechanistic studies of hydrogen release from solid amine borane materials. Mater Res Soc Symp Proc 2006;927(EE-02-04):0927.

[13] Bluhm ME, Bradley MG, Butterick R, Kusari U, Sneddon LG. Amineborane-based chemical hydrogen storage: enhanced ammonia borane dehydrogenation in ionic liquids. J Am Chem Soc 2006;128(24):7748-9.

[14] Wolf G, Baumann J, Baitalow F, Hoffmann FP. Calorimetric process monitoring of thermal decomposition of B-N-H compounds. Thermochim Acta 2000, 343(1-2):19-25.

[15] Satyapal S, Petrovic J, Read C, Thomas G, Ordaz G. The U.S. department of energy's national hydrogen storage project: progress towards meeting hydrogen-powered vehicle requirements. Catal Today 2007, 120(3-4):246-256.

[16] Denney MC, Pons V, Hebden TJ, Heinekey M, Goldberg KI. Efficient catalysis

of ammonia borane dehydrogenation. J Am Chem Soc 2006;128(37):12048–49.

[17] Stephens FH, Baker RT, Matus MH, Grant DJ, Dixon DA. Acid initiation of ammonia-borane dehydrogenation for hydrogen storage. Angew Chem Int Ed 2007;46(5):746–49.

[18] Gutowska A, Li L, Shin Y, Wang CM, Li XS, Linehan JC, Smith RS, Kay BD, Schmid B, Shaw W, Gutowski M, Autrey T. Nanoscaffold mediates hydrogen release and the reactivity of ammonia borane. Angew Chem Int Ed 2005; 44(23):3578–82.

[19] Bluhm ME, Bradley MG, Butterick R, Kusari U, Sneddon LG. Amineborane-based chemical hydrogen storage: enhanced ammonia borane dehydrogenation in ionic liquids. J Am Chem Soc 2006; 128(24):7748–49.

[20] Sepehri S, Feaver A, Shaw WJ, Howard CJ, Zhang QF, Autrey T, Cao GZ. Spectroscopic studies of dehydrogenation of ammonia borane in carbon cryogel. Journal of physical chemistry B 2007; 111: 14285-9.

[21] Feaver A, Sepehri S, Shamberger P, Stowe A, Autrey T, Cao GZ. Coherent carbon cryogel-ammonia borane nanocomposites for H2 storage. Journal of physical chemistry B 2007; 111:7469-72.

[22] Xiong Z, Yong CK, Wu G, Chen P, Shaw W, Karkamkar A, Autrey T, Jones MO, Johnson SR, Edwards PP, David WIF. High-capacity hydrogen storage in lithium and sodium amidoboranes. Nat Mater 2008;7:138-41.

[23] Wu H, Zhou W, Yildirim T. Alkali and alkaline-earth metal amidoboranes: structure, crystal chemistry, and hydrogen storage properties. J Am Chem Soc 2008; 130(44):14834-39.

[25] Kang XD, Ma LP, Fang ZZ, Gao LL, Luo JH, Wang SC, Wang P. Promoted hydrogen release from ammonia borane by mechanically milling with magnesium hydride: a new destabilizing approach. Phys Chem Chem Phys 2009, 11:2507-13.

[26] Kim DY, Lee HM, Seo J, Shin SK, Kim KS. Rules and trends of metal cation driven hydride-transfer mechanisms in metal amidoboranes. Phys Chem Chem Phys 2010, 12(20):5446-53.

[27] Luedtke AT, Autrey T. Hydrogen release studies of alkaline metal amidoboranes. Inorganic Chem 2010, 49(8):3905-10.

[28] Neiner D, Karkamkar A, Linehan JC, Arey B, Autrey T, Kauzlarich SM. Promotion of hydrogen release from ammonia borane with mechanically activated hexagonal boron nitride. J Phys Chem C 2009, 113(3):1098-1103.

[29] Diyabalanage HVK, Shrestha RP, Semelsberger TA, Scott BL, Bowden ME, Davis BL, et al. Calcium amidotrihydroborate: a hydrogen storage material. Angew Chem Int Ed 2007;46(47):8995-97.

Figure captions:

Fig. 1. TG (red line) and MS (green line, m/e = 2, H_2; blue line, m/e = 17, NH_3) profiles for MgH_2/AB (upper) and CaH_2/AB (lower) mixtures.

Fig. 2. XRD patterns for a) NH_3BH_3, b) MgH_2, c) ball milled MgH_2/AB mixture, d) MgH_2/AB mixture after heating (120 ºC), e) CaH_2, f) ball milled CaH_2/AB mixture, and g) CaH_2/AB mixture after heating (120 ºC).

Fig. 3. FT-IR spectra of MgH_2/AB (upper) and CaH_2/AB (lower) mixtures heated at different temperature (ºC).

Fig. 4. TG profiles for MgH_2/2AB (green line), MgH_2/3AB (blue line) and MgH_2/9AB (red line) mixture. MS profiles (top, m/e = 2, H_2; bottom, m/e = 17, NH_3) for MgH_2/2AB (green line), MgH_2/3AB (blue line) and MgH_2/9AB (red line) mixture. TG profiles for CaH_2/2AB (green line), CaH_2/3AB (blue line) and CaH_2/9AB (red line) mixture. MS profiles (top, m/e = 2, H_2; bottom, m/e = 17, NH_3) for CaH_2/2AB (green line), CaH_2/3AB (blue line) and CaH_2/9AB (red line) mixture.

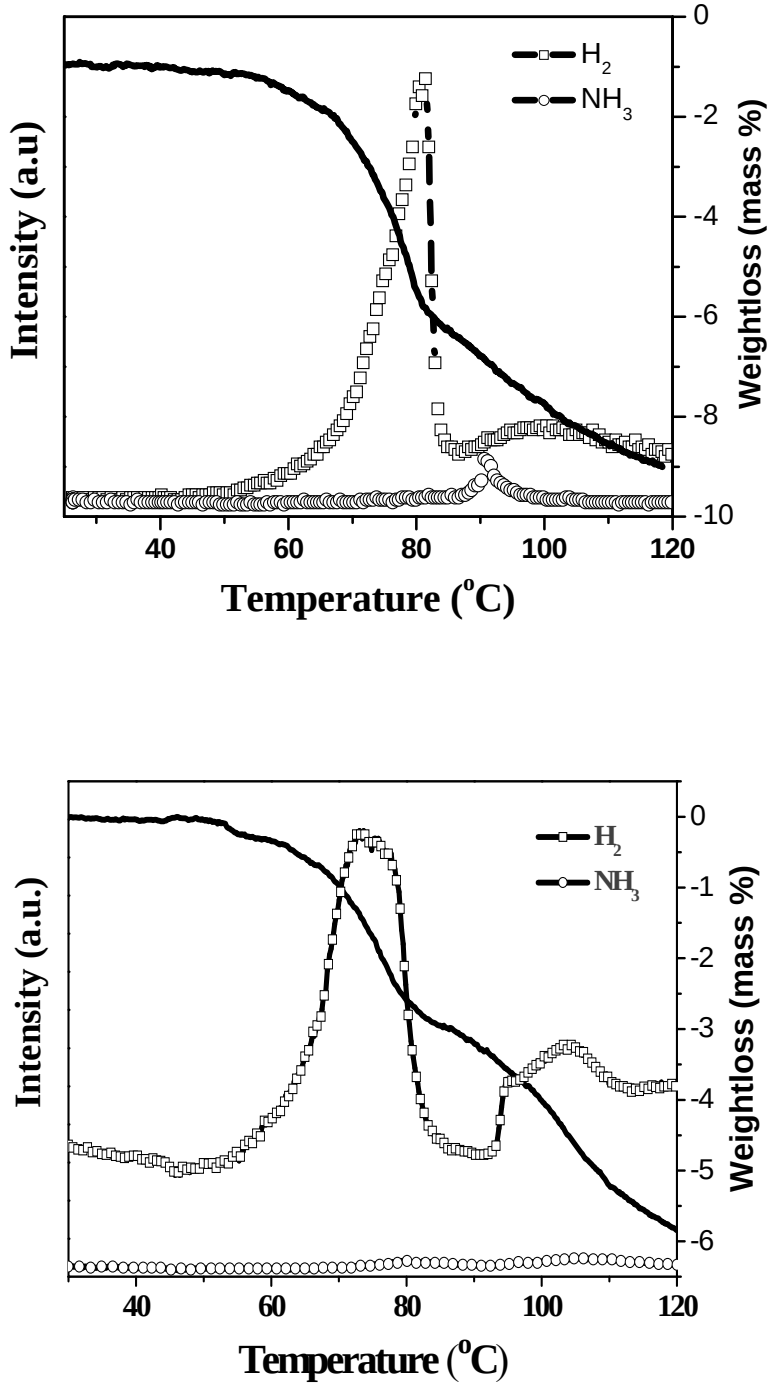

Fig. 1. TG (red line) and MS (green line, m/e = 2, H_2; blue line, m/e = 17, NH_3) profiles for MgH_2/AB (upper) and CaH_2/AB (lower) mixtures.

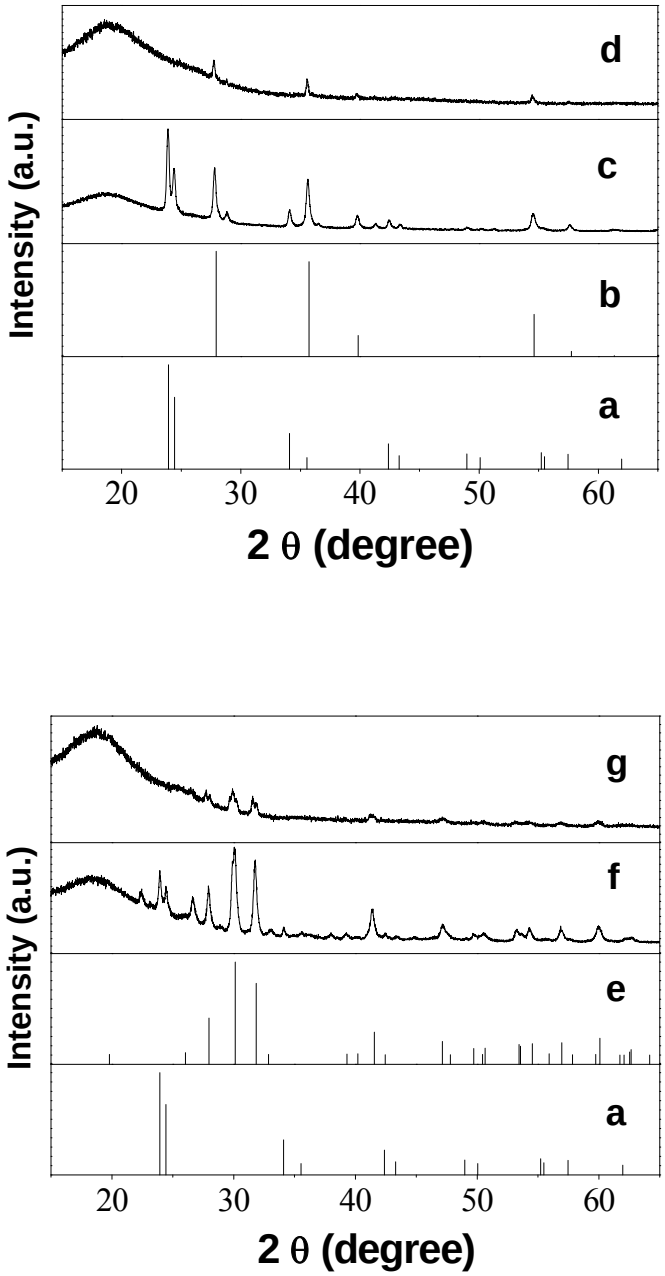

Fig. 2. XRD patterns for a) NH_3BH_3, b) MgH_2, c) ball milled MgH_2/AB mixture, d) MgH_2/AB mixture after heating (120 ºC), e) CaH_2, f) ball milled CaH_2/AB mixture, and g) CaH_2/AB mixture after heating (120 ºC).

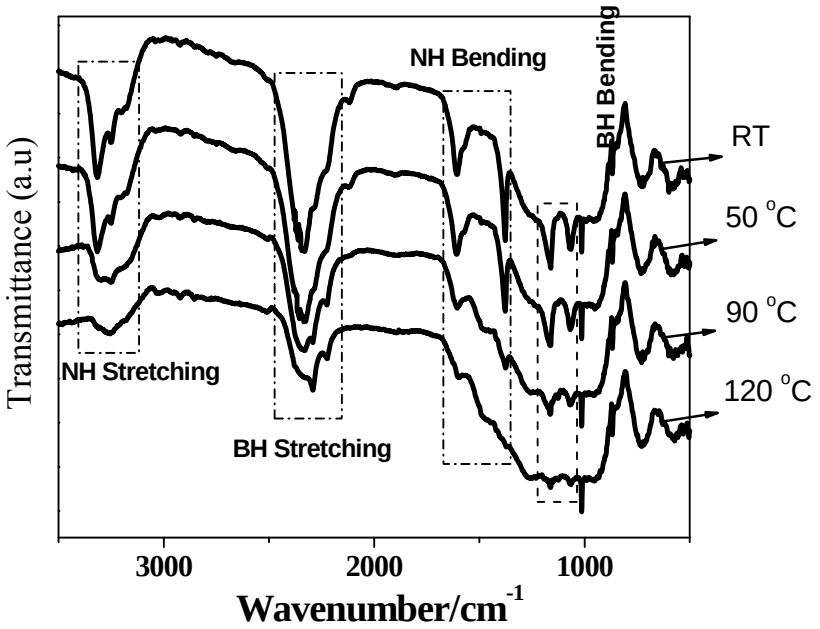

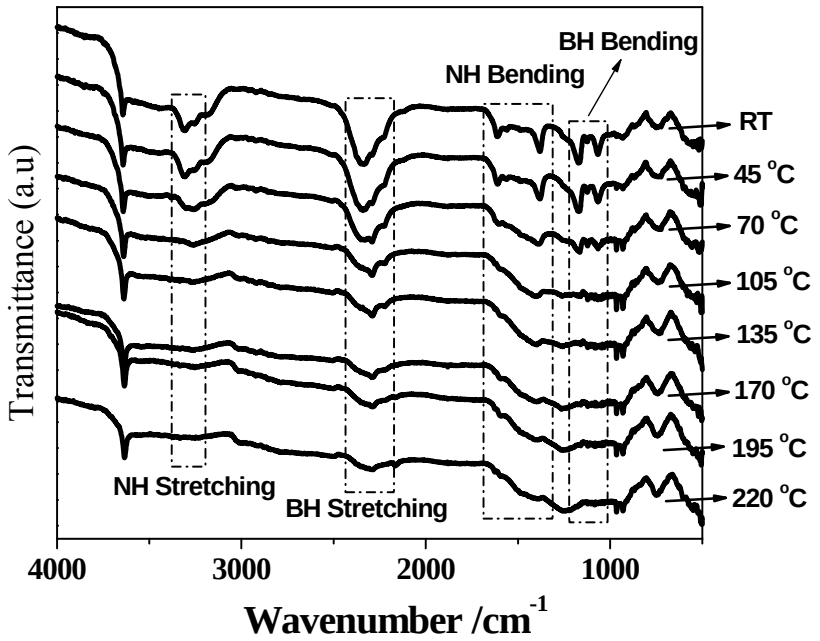

Fig. 3. FT-IR spectra of MgH_2/AB (upper) and CaH_2/AB (lower) mixtures heated at different temperature (ºC).

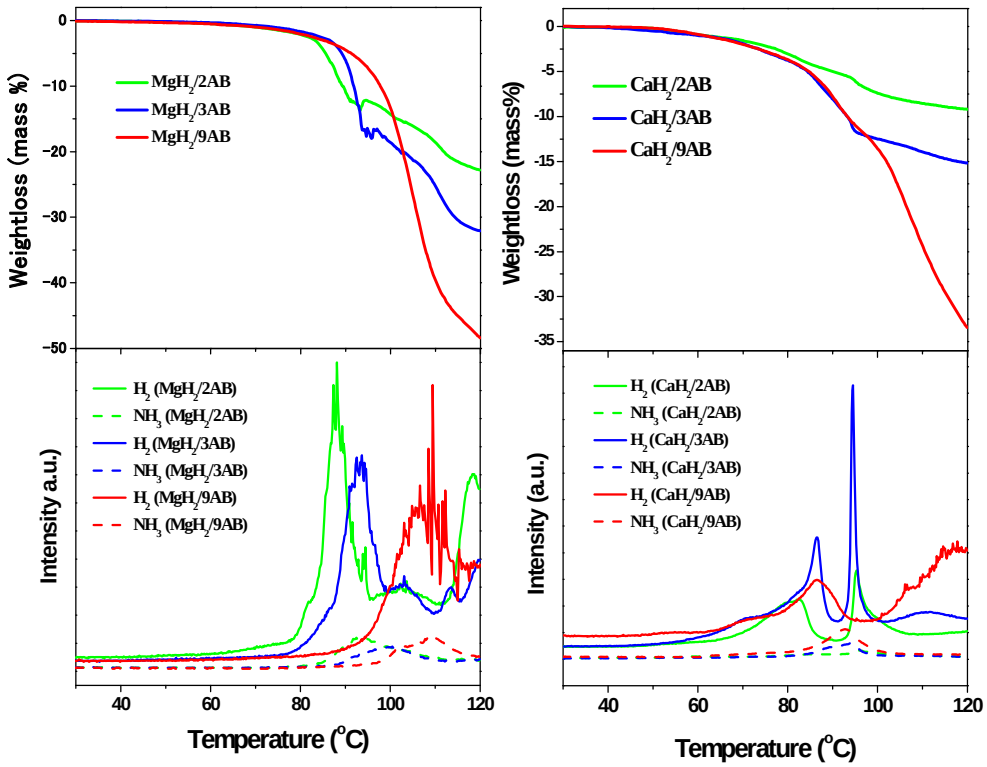

Fig. 4. TG profiles (left top) for MgH_2/2AB (green line), MgH_2/3AB (blue line) and MgH_2/9AB (red line) mixture. MS profiles (left bottom, solid line: m/e = 2, H_2; dash line: m/e = 17, NH_3) for MgH_2/2AB (green line), MgH_2/3AB (blue line) and MgH_2/9AB (red line) mixture. TG profiles (right top) for CaH_2/2AB (green line), CaH_2/3AB (blue line) and CaH_2/9AB (red line) mixture. MS profiles (right bottom, solid line: m/e = 2, H_2; dash line: m/e = 17, NH_3) for CaH_2/2AB (green line), CaH_2/3AB (blue line) and CaH_2/9AB (red line) mixture.